# Synthesis, Characterization and Biological Evaluation of New Dithiocarbamate Ligand and Its Complexes with some Metal Ions

**Ahmed T. Numan**
Dept. of Chemistry/ College of Education for Pure Science (Ibn Al-Haitham)/ University of Baghdad.
**Kaiss R. Ibraheem**
**Mohammed K. Ibrahim**
Dept. of Chemistry/ College of Science/ University of Anbar

**Received in:24/May/2017,Accepted in:6/September/2017**

## Abstract

New bidentate dithiocarbamate ligand (NaL) namely [Sodium-2-(((3-methyl -4- (2,2,2-tri fluoro ethoxy) pyridin-2 -yl) methyl) sulfinyl)-1H-benzoimidazole -1-carbodithioate] was prepared. This free ligand was synthesized from the reaction of a (RS)-2-([3-methyl -4-(2,2,2-tri fluoroethoxy) pyridin-2-yl] methyl sulfinyl)-1H benzoimidazole, $CS_2$ and NaOH in methanol as solvent. From reaction of dithiocarbamate salt (NaL) with metal ions (M); Co(II), Ni(II), Cu(II), Zn(II), Cd(II) and Pd(II) , have obtained the DTC complexes at general molecular formula $[M(L)_2(H_2O)_2]$ and $[Pd(L)_2]$. To characterize the ligand and its complexes, used different analyses methods such FTIR, UV-Vis, elemental microanalysis, atomic absoreption, magnetic susceptibility, conductance, melting points, $^1H$- $^{13}C$- NMR spectroscopy, thermal analysis and mass spectrum. These studies indicated the formation of DTC complexes which their geometries about metal centers are octahedral; except Pd-complex is square planer. The bacterial activity evaluation against investigated bacterial species indicated that the metal complexes are more active than the free ligand when compared them.

**Keywords:** Dithiocarbamate complexes; metal ions; Characterization; Bacterial activity.

https://doi.org/10.30526/30.3.1617

# Introduction

Dithiocarbamates (DTC) are organic compounds, which played an important role in the development of chemistry, especially in coordination chemistry field . This is due to strongly chelating ability towards metal ions [1,2]. The high ability of dithiocarbamates (DTC) to react with transition metals allowed them to be as useful ligands in both inorganic and bioinorganic chemistry. This is based on the sway of the anionic N-$CS_2^-$ moiety that has a variety of binding modes; mono, bi and bridging-dentate capable to form very stable complexes [3,4]. Interestingly, DTCs can be stabilised at a different oxidation states of metals, the compounds form and coordination geometries that show great structural diversities which range from monomeric to polymeric molecular [5,6]. The most common structural arrangements were the square planar and octahedral geometries [7]. The great applications are contributed considerably in developing the dithiocarbamates and their complexes, where included; Biomedical applications [8], analytical chemistry applications [9], environmental applications [10], agriculture applications and in the industry [11]. Also it investigates about the influence of dithiocarbamates against bacteria, fungi and microorganisms [12]. In this paper we report about synthesis, characterisation and bacterial evaluation of new dithiocarbamate ligand and its metal complexes.

# Experimental

All reagents used were analar or chemically pure grade by British drug house (BDH), Sigma-Aldrich,Merck and Fluka . Metal salts ($CoCl_2.6H_2O$, $NiCl_2.6H_2O$, $CuCl_2.2H_2O$, $ZnCl_2$, $CuCl_2.2H_2O$ and $PdCl_2$), (RS)-2-([3-methyl -4-(2,2,2-tri fluoroethoxy) pyridin-2-yl] methyl sulfinyl)-1H benzoimidazole, Carbon disulfide, DMSO, Ethanol and Methanol.

## Instrumentations

$^1$H and $^{13}$C-NMR were recorded using ultra shield 400 MHz Switzerland at Kharazmi University, Iran, conductivity measurements were carried out by Philips PW digital meters conductivity in DMSO at $10^{-3}$ M, FT-IR spectra were recorded as KBr discs in the range 4000-400 $cm^{-1}$ using Shimadzu 8300s FT-IR spectrophotometer and as CsI discs in the range 400-200 $cm^{-1}$ . UV-Visible spectra were recorded by Shimadzu UV-8300 vis160A ultraviolet spectrophotometer the range of (200-1100) nm at $10^{-3}$ M in DMSO . Metal contents of the complexes were determined by flame atomic absorption using (Shimadzu at A.A 680 GBC 933 plus) atomic absorption spectrophotometer, magnetic susceptibility (μeff. B.M) were recorded by faraday method using balance magnetic susceptibility model (Sherwood Scientific). Melting point was determined by using (Stuart-melting point apparatus). Determinations of (C, H, N and S) content for prepared compounds were carried out using Heraeus instrument (Vario EL) . Thermogravimetric analysis (TGA) was carried out using an STA PT-1000 Linseis company and mass spectrum by Shimadzu GC-Mass QPA-2013 spectrometer.

## Synthesis of free ligand

A standard method was used in the synthesis of dithiocarbamte compounds [13], it was used with a slight modifications to prepare the free ligand Sodium 2-(3-methyl-4-(2,2,2-trifluoroethoxy)pyridin-2-yl)methyl)sulfinyl)-1H-benzoimidazole-1-carbodithioate (NaL). Mixed equimolar amounts from reactors in following; (1 g, 2.70mmol) of (RS)-2-([3-methyl-4-(2,2,2-trifluoroethoxy)pyridin-2-yl] methylsulfinyl)-1H benzoimidazole was dissolved in 20ml of absolute methanol in a round bottom flask, then was added (0.10g, 2.70mmol) of sodium hydroxide dissolved in 2ml of double distilled water. The mixture was allowed to stir in a room temperature about 30 minutes and then was placed in ice bath. To this cold solution

https://doi.org/10.30526/30.3.1617

a pure carbon disulfide (0.163ml, 0.20g, 2.70mmol) was added drop-wise with constant stirring. The mixture was maintained at 0 °C for 4 h to result pale yellow solution then it was allowed at room temperature to evaporate, all of that was cleared in scheme (1). Sodium salt of dithiocarbamate was formed as a pale yellow powder, dried and recrystallized by methanol, washed several times by diethylether, decomposed at 201-203ºC. Yield: 66.67% and elemental microanalysis C.H.N. and S. were listed in Table(1) .

## Synthesis of $[Ni(L)_2(H_2O)_2]$ complex

A general method was used to achieve dithiocarbamate complexes[14,15] . A solution of (0.101g, 0.425mmol) $NiCl_2.6H_2O$ in 10ml ethanol was added drop wise to a round bottom flask, volume (100) ml, which contains a solution of (0.4g, 0.850mmol) of the dithiocarbamate ligand salt (NaL), dissolved in 10ml of ethanol. The reaction mixture was stirred and heated under reflux for 4 h, then was left to evaporate at room temperatures . The resulted solid washed with distilled water then by diethyl ether, dried at room temperature to give a pale green solid, m.p= 271 **ºC**. Yield: 0.242g (57.81%), Scheme (2) showed that.

## Synthesis of $[Co(L)_2(H_2O)_2]$, $[Cu(L)_2(H_2O)_2]$, $[Zn(L)_2(H_2O)_2]$, $[Cd(L)_2(H_2O)_2]$, $[Pd(L)_2]$ complexes.

A similar method to that mentioned in preparation of $[Ni(L)_2(H_2O)_2]$ complex with same quantitatives, was used to prepare NaL complexes with $CoCl_2.6H_2O$ (0.101g, 0.425mmol), $CuCl_2.2H_2O$(0.072g, 0.425mmol), $ZnCl_2$ (0.058g,0.425mmol), $CdCl_2.2H_2O$ (0.093g, 0.425mmol) and $PdCl_2$ (0.075g, 0.425mmol). Table (1) displays some physical properties of the prepared complexes, and elemental microanalysis C.H.N. and S. for some prepared complexes .

# Results and Discussion

The dithiocarbamate ligand (NaL) was synthesized in one step. The structure of (NaL) was checked and confirmed by elemental miocranalyses data (Table (1)), which is in good agreement with proposed formula $C_{17}H_{13}F_3N_3NaO_2S_3$ .

## IR Spectrum of the ligand (NaL)

The FTIR spectrum of Sodium2-(((3-methyl-4-(2,2,2trifluoroethoxy) pyridin-2-yl) methyl)sulfinyl)-1H-benzo[d]imidazole-1-carbodithioate(NaL) Figure (1), is compared with the FTIR spectra of the starting materials and carbon disulfide . The spectrum of NaL shows no band (disappeared) around 3222 $cm^{-1}$ was assigned to υ(NH) stretching vibration, compared with that observed in the starting material [16] . The IR spectrum reveals new band at 1446 $cm^{-1}$ can be attributed to υ(C-N) stretching of ($N\text{-}CS_2$) moiety [17] . Also the IR spectrum reveals two new bands at 1055 $cm^{-1}$ and 942 $cm^{-1}$ attributed to $\upsilon_{asy}$ ($CS_2$) and $\upsilon_{sy}$ ($CS_2$), respectively [18] . The bands at 3062 $cm^{-1}$ and 2990, 2943 $cm^{-1}$ attributed to the υ(C–H) aromatic and υ(C–H) aliphatic stretching vibration respectively . The bands observed at 1630 $cm^{-1}$ and 1587$cm^{-1}$ were assigned to υ (C=N) and $\upsilon_{aromatic}$(C=C) mode of aromatic system respectively [19]. While the band observed at 1271 $cm^{-1}$ recorded to υ (C–N) stretching vibration [20]. On the other hand the spectrum displayed bands at 1188 $cm^{-1}$, 972 $cm^{-1}$ and 663 $cm^{-1}$ attributed to the υ(C–O–C), υ(C–S) and υ(C–F) respectively [21]. The assignments of characteristic bands are summarized in Tables (2).

## Electronic Spectrum of the ligand (NaL)

The U.V-Vis spectrum of ligand NaL in DMSO solution, Figure (2) showed two absorption peaks, the first peak at (285 nm =35087 $cm^{-1}$; $\varepsilon_{max}$= 2401$molar^{-1}$ $cm^{1}$) was assigned to $\pi \rightarrow \pi^*$

https://doi.org/10.30526/30.3.1617

electronic transition. The second peak at (321 nm =31152 cm$^{-1}$; $\varepsilon_{max}$= 1728 molar$^{-1}$ cm$^{-1}$) was attributed to n→π* electronic transition [22,23]. The U.V-Vis spectral data of the ligand (NaL) were given in Table (3).

## $^{1}$H, $^{13}$C-NMR spectra for the ligand (NaL)

The $^{1}$H-NMR spectrum for the ligand NaL in Figure (3) showed the following characteristic chemical shift (DMSO-d$^{6}$ as a solvent) : The spectrum showed the singlet signal at δ=8.35 ppm is assigned to proton for $C_{14}$. The singlet chemical shifts at δ=7.57 ppm and 7.55 ppm are assigned to protons for $C_7$ and $C_4$ respectively. The signal at chemical shift δ=7.54 ppm is assigned to the proton for $C_{15}$. The multiple chemical shifts at δ=7.10 ppm and 7.09 ppm refers to the protons of the $C_6$ and $C_5$ respectively. A signal at δ= 4.54 ppm attributed to the two protons for $C_{19}$ of methylene group, While a multiple signal at δ= 4.36 ppm attributed to the two protons for $C_{11}$ of another methylene group. The chemical shift at δ=2.51 is assigned to DMSO solvent. The chemical shift at δ=2.19 is assigned to the three protons for $C_{18}$ of methyl group. The NMR spectral data of ligand was reported in literatures [24,25].

The $^{13}$C-NMR spectrum of a ligand NaL, Figure (4) in DMSO-d$^{6}$ solvent showed that the chemical shift at δ= 192.3 ppm attributed to carbon atom $C_{10}$ for S=C-S of dithiocarbamate group [4]. The carbon atoms $C_{16}$ and $C_{12}$ resonated with the chemical shifts at δ= 161.2, 160.1 ppm respectively. The carbon atom $C_{14}$ resonated with the chemical shift at δ =152.4 ppm. The carbon atoms $C_2$, $C_9$ and $C_8$ resonated with the chemical shifts at δ = 148.0, 144.7 and 127.9 ppm respectively. The carbon atoms $C_5$ and $C_6$ resonated with the chemical shift at δ = 125.1 ppm. The carbon atom $C_{20}$ of C-$F_3$ group resonated with the chemical shift at δ =122.4 ppm. Also the carbon atoms $C_4$ and $C_7$ resonated with the chemical shifts at δ=121.9, 119.5 ppm respectively. While the carbon atoms $C_{17}$, $C_{15}$ resonated with the chemical shifts at δ= 117.0, 106.7 ppm respectively. The carbon atom $C_{19}$ for C-O resonated with the chemical shift at δ= 73.8 ppm, While the carbon atom $C_{11}$for C-S=O resonated with the chemical shift at δ= 60.1 ppm. The chemical shift at δ=40.06 ppm attributed to DMSO solvent. Finally the chemical shift at δ =10.5 ppm attributed to the carbon atom $C_{18}$ of methyl group. The $^{13}$C-NMR spectral data of ligand was reported in literatures [9,26].

## Mass Spectrum of the ligand (NaL)

The electrospray (+) mass spectrum of NaL is exhibited successive fragments related to ligand s'tructure . The parent ion peak for the ligand is observed at m/z = 467.6 which corresponds to $M^+$ (15%) for $C_{17}H_{13}N_3NaO_2S_3F_3$; requires = 467.4. The other peak fragments are shown in Figure (5).

## The IR Spectra for the DTC Complexes

The FTIR spectrum of $[Co(L)_2(H_2O)_2]$, Figure (6), exhibits bands related to the ligand with the appropriate shift due to complex formation . “The spectrum displays band at 1629 cm$^{-1}$, which is related to $\nu$(C=N) moiety, when the band at 1587 cm$^{-1}$ was assigned to $\nu_{ar}$(C=C) modes of aromatic system . Also the spectrum was displayed band at 1469 cm$^{-1}$, which is related to $\nu$(N-$CS_2$) mode, compared with that detected in the free ligand at 1446 cm$^{-1}$ . The complex exhibited two bands, which are attributed to the asymmetric $\nu$($CS_2$) at1055 cm$^{-1}$ and symmetric $\nu$($CS_2$) at 942 cm$^{-1}$ stretching . These bands are characteristic for an anisobidentate chelating mode of the ligand to the metal ions[27,28] . At lower frequency (far FTIR) complex $[Co(L)_2(H_2O)_2]$, exhibited two bands at 393cm$^{-1}$ and 375cm$^{-1}$ that are assigned to the ν(M-S) vibrational mode and supporting the anisobidentate chelation mode of the ligand [27] . The $\nu_{ar}$(C-H) stretching of the aromatic ring which occurs slightly above 3000 cm $^{-1}$ is observed at 3068 cm$^{-1}$, when the ν(C-H) stretching for the aliphatic group is

https://doi.org/10.30526/30.3.1617

detected at 2939 $cm^{-1}$ [19]. Also the IR spectrum exhibited broad band at 3471$cm^{-1}$ and new' band at 816$cm^{-1}$ that may be attributed to υ(OH) and δ(OH) respectively which refer to coordinated $H_2O$ molecule (aqua) with Co-complex in molecular formula [29]. The FTIR spectra for $[Ni(L)_2(H_2O)_2]$, $[Cu(L)_2(H_2O)_2]$, $[Zn(L)_2(H_2O)_2]$, $[Cd(L)_2(H_2O)_2]$ and $[Pd(L)_2]$ complexes, Figures (7) show similar trend to that of the $[Co(L)_2(H_2O)_2]$ complex and same reasoning could be used to interpret the spectrum, all the results are summarized in table (2).

## The Electronic Spectra and Magnetic Studies for the DTC Complexes

The electronic spectrum of $Co^{II}$-complex, exhibits five peaks, The first and second peaks at (279 nm=35842 $cm^{-1}$) and (353 nm= 28328$cm^{-1}$) were assigned to the ligand field (L.F), while the third peak at(401 nm=24937 $cm^{-1}$) is due to charge transfer transition. The peaks at visible region (d-d) at (565 nm=17699 $cm^{-1}$), (724 nm=13812 $cm^{-1}$) due to the d-d electronic transition typ ($^4T_1g_{(F)}\rightarrow{}^4T_1g_{(P)}$) and ($^4T_1g_{(F)}\rightarrow{}^4A_2g_{(F)}$) respectively, transitions confirming an octahedral structure around Co(II) central metal ion [30]. The magnetic susceptibility measurement for the solid Co(II) complex is (4.86) B.M. also is indicative of three unpaired electron per Co(II) ion suggesting consistency with its octahedral environment[31].

The electronic spectrum of Ni-complex showed peaks in the (281nm=35587 $cm^{-1}$) and (352 nm= 28409$cm^{-1}$) were assigned to the ligand field. And another peak in the (390nm=25641 $cm^{-1}$) due to charge transfer transition. And the peaks at visible region at (837 nm=11947 $cm^{-1}$) and (937nm=10672 $cm^{-1}$) due to the d-d electronic transition. These peaks are assigned to ($^3A_2g\rightarrow{}^3T_1g_{(P)}$) and ($^3A_2g\rightarrow{}^3T_2g_{(F)}$) respectively, transitions confirming an octahedral structure around Ni (II) ion complex [32]. The magnetic susceptibility measurement for the solid Ni(II) complex is (2,9) B.M. also is indicative of two unpaired electrons per Ni (II) ion suggesting consistency with its octahedral geometry[31].

The electronic spectrum of Cu-complex showed two peaks in the range (274 nm=36496 $cm^{-1}$) and (352nm=28409 $cm^{-1}$) are assigned to the ligand field. And another peak in the range (371 nm=26954 $cm^{-1}$) is due to charge transfer transition. The peak at visible region at (722 nm=13850$cm^{-1}$) is due to the d-d electronic transition type.”This peak is assigned to ($^2Eg\rightarrow{}^2T_2g$) transition confirming a distorted octahedral structure around Cu(II) ion complex [33]. The magnetic susceptibility measurement of Cu(II) complex is (1.89) B.M., which suggests the presence of one unpaired electron with its octahedral environment[31].

The electronic spectral of $Zn^{II}$-and $Cd^{II}$- complexes. In each case the spectrum showed three intense peaks in the U.V region at (274nm=36496$cm^{-1}$, 368nm=27173$cm^{-1}$) and (277nm=36101$cm^{-1}$, 347nm=28818$cm^{-1}$) for $Zn^{II}$ and $Cd^{II}$ - complexes respectively, assigned to the ligand field. While the peaks at (406nm=24630$cm^{-1}$) and at (401nm=24937$cm^{-1}$) are assigned to the charge transfer transitions. Finally the metal ion of these complexes belongs to $d^{10}$ system and these metals do not show d–d transition. These complexes are diamagnetic as expected and it showed octahedral geometries [34,35].

The electronic spectrum of Pd-complex, Figure (8) showed two peaks in the range (302 nm=33112 $cm^{-1}$) and (345nm=28989$cm^{-1}$) are assigned to the ligand field. And another peak in the range (380 nm=26315 $cm^{-1}$) due to charge transfer transition. The peaks at visible region at (719 nm=13908$cm^{-1}$) and (804 nm=12437$cm^{-1}$) due to the d-d electronic transition type. These peaks are assigned to ($^1A_1g\rightarrow{}^1B_1g$) and ($^1A_1g\rightarrow{}^1E_1g$) respectively, transitions confirming a square planer structure around Pd(II) ion complex, This complex is diamagnetic [36]. Electronic spectral data and magnetic susceptibility for these complexes are summarised in table (3)

https://doi.org/10.30526/30.3.1617

## Thermal analysis

The thermal analysis curve (TGA) for $[Cd(L)_2(H_2O)_2]$ is shown in Figure (9). The thermogram revealed that the complex is stable up to 78°C in helium atmosphere. It is decompose in four steps. The first step observed at 78.4-193°C attributed to the loss of $(2H_2O)$ fragment, (obs.= 0.5700 mg, 3.00%; calc.= 0.6594 mg, 3.471%). The second step occurred at 193-319°C indicated to the loss of $(C_{14}H_{11}N_3OS_2F_3+CS_2)$ fragment, (obs.= 8.1624 mg, 42.96%; calc.= 7.9515mg, 41.85%) . The third step occurred at 319-415°C indicated to the loss of $(C_{12}H_8NOF_3+CS_2)$ fragment, (obs.= 5.6335 mg, 29.65%; calc.= 5.8387mg, 30.73%) . The fourth step found at 415-578°C indicated to the loss of $(C_6H_7N_2O)$ fragment, (obs.= 2.4795 mg, calc.= 16.703 mg, 87.912%) while, the residue of the compound is related to the (CdO), (obs.= 2.5346 mg, 13.34%; calc.= 2.2967mg, 12.09%)[37,38]. Thermal decomposition data for this complex is summarized in table (4).

## Molar Conductivity

The molar conductance values of the the complexes in DMSO lie in the range (8.2-18) $ohm^{-1}.cm^2.mol^{-1}$which is quite lower than that expected for an electrolyte and reveal their nonelectrolyte nature [9] as in table (1).

## Bacterial activity

The synthesised dithiocarbamate ligand (NaL) and its metal complexes were tested by using disc method inhibition (against four types of pathogenic bacteria, *Escherichia coli and Pseudomonas aeruginosa* (G−) that gram negative, *Staphylococcus aureus and Bacillus stubtilis* (G+) that gram positive. Data of the measured inhibition zones against growth of different bacteria's are summarised in Table (5), which displays the effect of the synthesised compounds on bacterial strains. From obtained data, it is obvious that, the complexes are already more active against these bacterial specie compared with the free ligand, which means complexation increases antimicrobial activity.

## Conclusion

The new dithiocarbamate ligand (NaL) and its metal complexes were aprepared by the mixing of the DTC ligand with metal ion to form the following formula;$[Co(L)_2(H_2O)_2]$, $[Ni(L)_2(H_2O)_2]$, $[Cu(L)_2(H_2O)_2]$, $[Zn(L)_2(H_2O)_2]$ $[Cd(L)_2(H_2O)_2]$ and $[Pd(L)_2]$, where metal (II) ions are coordinated by sulfur atoms. Magnetic tests and Spectroscopic data prove that all complexes are octahedral geometries, except palladium complex shows square planer geometry as expected. The biological evaluation against bacterial species indicated that the metal complexes are more active than the free ligand.

## References

1. Nami, S. A.; Ullah, I.; Alam, M.; Lee, D-U. and Sarikavakli, N.,(2016). "Synthesis, characterization, molecular docking and biological studies of self -assembled transition metal dithiocarbamates of substituted Pyrrole-2-Carboxaldehyde", J. of Photochem.and Photobio. B: Biology, 160. 392-399.
2. Kanchi, S.; Singh, P. and Betty, (2014). "Dithiocarbamates as hazardous remediation agent: A critical review on progress in environmental chemistry for inorganic species studies of the 20th century", Arabian J. of Chemistry, 7. 11–25.

https://doi.org/10.30526/30.3.1617

3. Baba, I.; Raya, I. and Yamin, B. M.,(2009). “Synthesis and structural studies of lanthanum (Iii) dialkyldithiocarbamates 1,10-phenantroline”, J. Sains Malaysiana, 38(2). 185-190.
4. Al-Fahdawi, A. S. M., (2013) “Formation of bimetallic bis(dithiocarbamate) macrocyclic complexes”., PH.D thesis, Babylon University, College of science, 1-242.
5. Yih, K.-H.; Chen, S.-C.; Lin, Y.-C.; Lee G.-H. and Wang, Y.,(1995). “New syntheses of [Et$_4$N][(C$_5$H$_{10}$NCS$_2$)M(CO)$_4$](M= Cr, Mo and W):Insertion reaction of carbon disulfide into the metal-nitrogen bond”., J. Organo met. Chem., 494.149-155.
6. Edwards, A.; Hogarth, G.; Hollingsworth, N. and Oller, J. J.; (2011). “Illusive tungsten-imido-dithiocarbamate complexes: Facile carbon-nitrogen bond formation”, J.Inorg. Chem. Commun.,14.1932-1936.
7. Plyusnin, V.F.; Grivin, V.P. and Larionov, S.V.,(1997). “Photochemistry of Fe(III), Fe(IV), Ru(III), Mo(VI), and Ni(IV) dithiocarbamate complexes”., J.Coord. Chem. Rev.,159.121-133.
8. Ozturk, B. C. N.; Kourkoumelis, N.; Manos, M. J.; Tasiopoulos, A. J.; Owczarzak, A. M.; Kubicki, M. and Hadjikakou, S. K., (2014). “Synthesis, characterization and biological activity of antimony(III) or bismuth(III) chloride complexes with dithiocarbamate ligands derived from thiuram degradation”, J. Polyhedron., 67. 89–103
9. Hasan, A. H.and Yousif, E. I., (2016). “Formation of new macrocyclic complexes with bis (dithiocarbamate) ligand; preparation, structural characterisation and bacterial activity”, *Ibn Al-Haitham* J. for Pure & Appl. Sci., 29(3).146-166.
10. Figueira, P.; Lopes, C. B.; Danieli-da-silva, A. L.; Pereira, E.; Duarte, C. and Trindad, T.,(2011). “Removal of mercury (II) by dithiocarbamate surface functionalized magnetite particles: application to synthetic and natural spiked waters”, Water Res., 45(17). 5773-5784.
11. Damicone, J.; (2016). “Fungicide resistance management., division of agricultural sciences and natural resources”., Oklahoma State Univ., EPP-7663.1-8.
12. Ekennia, A. C.; Onwudiwe, D. C; Ume, C. and Ebenso, E. E.,(2015). “Mixed ligand complexes of N-methyl-N-phenyldithiocarbamate: synthesis, characterisation, antifungal activity, and solvent extraction studies of the ligand”,J. Bioinorg.Chem.& Appl., 2015.1-10.
13. Martínez, J. A.; Valenzuela, J. and Hernandez-Tamargo, C. E., (2015). “Study of sulfur adlayers on Au (111) from basic hydrolysis of piperazine bis (dithiocarbamate) sodium salt”, J. Appl. Surf. Sci., 345. 394-399.
14. Ingle, A. D.; Devghare, H. and Parase, K.,(2013). “Metal complexes of ammonium phenyl dithiocarbamate: Preparation characterization and biological activity”. J. Chem. Pharm. Res., 5(7). 272-277.
15. Kumar, V.; Singh, V.; Gupta, A. N.; Manar, K. K.; Drew, M. G.and Singh, N., (2014). “Influence of ligand environments on the structures and luminescence properties of homoleptic cadmium (II) pyridyl functionalized dithiocarbamates”, J.Cryst. Eng. Comm.,16(29). 6765-6774.
16. Biancalana, L.; Bresciani, G.; Chiappe, C.; Marchetti, F. and Pampaloni,G., (2017). “Synthesis and study of the stability of amidinium/guanidinium carbamates of amines and α-amino acids”,New J. Chem., 41(4). 1798-1805.
17. Faraglia, G.; Sitran, S. and Montagner, D., (2005). “Pyrrolidine dithiocarbamates of Pd(II)”, J. Inorg. Chim. Acta., 358. 971-980.
18. Yin, D.; Zhai, J.; Sun, Y-Y. and Wang, D-Q., (2008). “Synthesis, characterizations and crystal structures of new antimony (III) complexes with dithiocarbamate ligands”, J.Polyhedron, 27(2). 663-670.
19. Podunavac-Kuzmanovic, S. O.; Cvetkovic, D. M.and Vojinovic, L. S., (2004). “Synthesis, physico-chemical characterization and biological activity of 2-

https://doi.org/10.30526/30.3.1617

aminobenzimidazole complexes with different metal ions", J.Acta Periodica Technologica, 35. 239-246.

20. Nagarajua, M.; Bandichhora, R. and Mukkantib, K.,(2013). "Identification, synthesis and characterization of potential impurities of dexlansoprazole", J. Chem. Bio.Interface, 3(6). 366-374.
21. Reddy, B. R. L.; Raju, K. N. and Eswaraiah, M. C., (2012). "Formulation and evaluation of controlled release microspheres of lansopprazole"., Int. Res. J. Pharm. App. Sci., 2(6). 90-96.
22. Orescanin, V.; Mikelic, L.; Roje, V. and Lulic, S., (2006). "Determination of lanthanides by source excited energy dispersive X-ray fluorescence (EDXRF) method after preconcentration with ammonium pyrrolidine dithiocarbamate(APDC)", J. Analytical Chimica Acta, 570.2. 277-282.
23. Ronconi, L.; Giovagnini, L.; Marzona, C.; Bettio, F.; Graziani, R.; Pilloni, G. and Fregona, D.; (2005). "Gold dithiocarbamate derivatives as potential antineoplastic agents:Design, spectroscopic properties, and in vitro antitumor activity", J. Inorg. Chem., 44.6. 1867-1881.
24. Tamizmani, M.; Kankanala, R. and Sivasankar, C., (2014). "Coordinated and uncoordinated anion dictated coordination mode of PN(Me)P ligand in Pd(II) complexes and their catalytic applications", J. Organomet. Chem., 6 (12). 763-764.
25. Pai, N. R. and Patil, S. N. S., (2014). "synthesis of lansoprazol impuritiesby conventional method", Inter. J. Med. Chem. Anal., 4(2).116-120.
26. Singh, G. S. and Pheko, T., (2008) "Spectroscopic characterization of the 1-substituted 3,3'-diphenyl-4-(2'-hydroxyphenyl)azetidine-2-ones: applic- ation of $^{13}$C NMR, $^{1}$H NMR and mass spectroscopy", J. Spectrochim. Acta, Part A, 70. 595-600.
27. Loveness, B. N.,(2015). "Copper dithiocarbamate complexes and copper sulphide nanaparticales: synthesis, characterization and antifungal Studies", M. Sc. Thesis, University of Fort Hare, 31-76.
28. Siddiqi, K. S.; Nami, S. A. A.; Lutfullaha and Chebudeb, Y., (2006) "Template synthesis of symmetrical transition metal dithiocarbamates", J. Braz. Chem. Soc., 17(1). 107-112.
29. Nakamoto, K.; (1997). "Infrared and Raman Spectra of Inorganic and Coordination Compounds", Parts A and B, 5th ed., John Wiley Sons, New York.
30. Tiwari, S.; Raddey, K. V.; Bajpai, A.; Khare, K.and Nagaraju, V., (2015). "Synthesis and Characterization of Bisdithiocarbamates from Weak Nitrogen Bases and Its Metal Complexes", Inter. Res. J. Pure &Appl. Chem., **7**(2).78-91.
31. Housecroft, C. E. and Sharpe, A. G., (2008). "Inorganic Chemistry", 3rd Ed., Pearson Education Limited: Essex, England, 573-681.
32. Nami, S. A.; Husain, A. and Ullah, I., (2014). "Self- assembled homodinuclear dithiocarbamates: One pot synthesis and spectral characterization", J. Spectrochimica Acta Part A: Mol. Bio Spectroscopy.,118. 380-388.
33. Lever, A. B. P., (1984). "Inorganic Electronic Spectroscop", 2nd.Ed., Elsevier publisher, NewYork.
34. Alyass, J. M. and Mohammed, A. F., (2012). "Synthesis and characterization of Co(II) , Ni(II), Cu(II) Zn(II) and Cd(II) mixed complexes of imidazol dithiocarbamate and 1,10-phenanthroline"., Iraqi Nat. J. Chem., 45.105- 116.
35. Shriver, D.W. and Atkins, P.W., (2006). "Inorganic chemistry, electronic spectra of TM complexes". 4th ed. Freeman, New York.
36. Karcz, D.; Matwijczuk, A.; Boron, B.; Creaven, B.; Fiedor, L.; Niewiadomy, A. and Gago, M., (2017)."Isolation and spectroscopic characterization of Zn(II), Cu(II), and Pd(II) complexes of 1,3,4 thiadiazole-derived ligand", J. Molec. Struc., 1128. 44-50.

https://doi.org/10.30526/30.3.1617

37. Al-Hamdani, A. A. S.and Hamodha, R. G., (2016). "Transition metal complexes with tridentate ligand: preparation, spectroscopic characterization, thermal analysis and structure studies", J. Bag. Sci., 13(4). 770-781.
38. Al Zoubi, W.; Al-Hamdani, A. A. S. and GunKo, Y.,(2017). "Schiff bases and their complexes: Recent progress in thermal analysis", J. Separation Sci.Tech., 52(6). 1052-1069.

**Table (1): Colours, yields, melting points, (C, H, N, S) analysis and molar conductance values for ligand and its dithiocarbamate complexes**

| Comp. | M.wt g\mol | m.p ºC | Yield % | Colour | ʌm $S.Cm^2$ $molar^-$ | Microanalysis Found (calc) % | | | | |
|---|---|---|---|---|---|---|---|---|---|---|
| | | | | | | M% | C | H | N | S |
| NaL | 467.47 | 201-203* | 66.67 | Pale yellow | - | - | 43.09<br>(43.68) | 2.43<br>(2.80) | 9.74<br>(8.99) | 20.01<br>(20.57) |
| $[Co(L)_2(H_2O)_2]$ | 983.93 | 282* | 55.25 | Green | 18.0 | 5.87<br>(5.99) | (41.50) | (3.07) | (8.54) | (19.55) |
| $[Ni(L)_2(H_2O)_2]$ | 983.69 | 271 | 57.81 | Pale green | 15.7 | 5.57<br>(5.97) | 40.83<br>(41.51) | 2.91<br>(3.07) | 8.79<br>(8.54) | 19.34<br>(19.55) |
| $[Cu(L)_2(H_2O)_2]$ | 988.55 | 279 | 61.36 | Brown | 10.9 | 6.58<br>(6.43) | (41.31 | (3.06) | (8.50) | (19.46) |
| $[Zn(L)_2(H_2O)_2]$ | 990.38 | 290* | 48.74 | White | 8.9 | 6.01<br>(6.60) | 41.06<br>(41.23) | 2.98<br>(3.05) | 8.41<br>(8.49) | 18.85<br>(19.42) |
| $[Cd(L)_2(H_2O)_2]$ | 1037.4 | 326* | 63.09 | Yellow white | 8.2 | 10.81<br>(10.84) | (39.36) | (2.91) | (8.10) | (18.54 |
| $[Pd(L)_2]$ | 995.39 | 296* | 59.06 | Brown | 16.3 | 10.43<br>(10.69) | 40.77<br>(41.03) | 2.51<br>(2.63) | 8.73<br>(8.44) | 18.41<br>(19.33) |

*= decompose

**Table (2): FT-IR data (wave-number) $cm^{-1}$ of ligand and its metal complexes.**

| Comp. | ν(OH) water | $ν_{arom}$ (C-H) | $ν_{alip}$ h(C-H) | ν(C=N) | $ν_{ar}$ (C=C) | ν(N-$CS_2$) | ν(C-N) | ν(C-O-C) | νas($CS_2$)<br>ν,s($CS_2$) | ν($H_2O$) | ν(M-O) |
|---|---|---|---|---|---|---|---|---|---|---|---|
| Starting materials | _ | 3066 | 2983<br>2927 | 1631 | 1583 | _ | 1275 | 1173 | _ | _ | _ |
| NaL | _ | 3062 | 2990<br>2943 | 1630 | 1587 | 1446 | 1271 | 1188 | 1055<br>942 | _ | _ |
| $[Co(L)_2(H_2O)_2]$* | 3471 | 3068 | 2939 | 1629 | 1587 | 1469 | 1261 | 1173 | 1101<br>914 | 816 | 607 |
| $[Ni(L)_2(H_2O)_2]$ | 3439 | 3032 | 2966 | 1627 | 1591 | 1473 | 1261 | 1173 | 1109<br>922 | 820 | 611 |
| $[Cu(L)_2(H_2O)_2]$ | 3437 | 3078 | 2976 | 1631 | 1579 | 1470 | 1259 | 1170 | 1086<br>916 | 814 | 621 |
| $[Zn(L)_2(H_2O)_2]$ | 3444 | 3086 | 2972 | 1622 | 1579 | 1456 | 1275 | 1173 | 1113<br>915 | 827 | 619 |
| $[Cd(L)_2(H_2O)_2]$ | 3440 | 3070 | 2951 | 1647 | 1591 | 1464 | 1263 | 1176 | 1082<br>928 | 825 | 580 |
| $[Pd(L)_2]$ | _ | 3080 | 2966<br>2931 | 1633 | 1581 | 1477 | 1257 | 1169 | 1047<br>918 | _ | _ |

https://doi.org/10.30526/30.3.1617

* υ(M–S) observed at $393 cm^{-1}$ and $375 cm^{-1}$

**Table (3): UV-Vis spectral data of ligand and dithiocarbamate complexes in DMSO solutions and magnetic moment**

| Compound | Wavenumber | | $\varepsilon_{max}$ $molar^{-1}cm^{-1}$ | Assignment | Suggested structure | μeff (B.M) |
|---|---|---|---|---|---|---|
| | nm | $Cm^{-1}$ | | | | |
| NaL | 285 | 35087 | 2401 | $\pi\rightarrow\pi^*$ | – | – |
| | 321 | 31152 | 1728 | $n\rightarrow\pi^*$ | | |
| $[Co(L)_2(H_2O)_2]$ | 279<br>353 | 35842<br>28328 | 2395<br>569 | L.F<br>L.F | Oh | 4.86 |
| | 401 | 24937 | 365 | C.T | | |
| | 565<br>724 | 17699<br>13812 | 34<br>32 | $^4T_1g_{(F)}\rightarrow{}^4T_1g_{(P)}$<br>$^4T_1g_{(F)}\rightarrow{}^4A_2g_{(F)}$ | | |
| $[Ni(L)_2(H_2O)_2]$ | 281<br>352 | 35587<br>28409 | 2435<br>637 | L.F<br>L.F | Oh | 2.90 |
| | 390 | 25641 | 232 | C.T | | |
| | 837<br>937 | 11947<br>10672 | 10<br>12 | $^3A_2g\rightarrow{}^3T_1g_{(P)}$<br>$^3A_2g\rightarrow{}^3T_2g_{(F)}$ | | |
| $[Cu(L)_2(H_2O)_2]$ | 274<br>352 | 36496<br>28409 | 2230<br>731 | L.F<br>L.F | distorted Oh | 1.89 |
| | 371 | 26954 | 484 | C.T | | |
| | 722 | 13850 | 23 | $^2Eg\rightarrow{}^2T_2g$ | | |
| $[Zn(L)_2(H_2O)_2]$ | 274<br>368 | 36496<br>27173 | 2264<br>1361 | L.F<br>L.F | Oh | Diamagnetic |
| | 406 | 24630 | 392 | C.T | | |
| $[Cd(L)_2(H_2O)_2]$ | 277<br>347 | 36101<br>28818 | 2424<br>406 | L.F<br>L.F | Oh | Diamagnetic |
| | 401 | 24937 | 171 | C.T | | |
| $[Pd(L)_2]$ | 302<br>345 | 33112<br>28985 | 2121<br>2188 | L.F<br>L.F | Sp | Diamagnetic |
| | 380 | 26315 | 1231 | C.T | | |
| | 719<br>804 | 13908<br>12437 | 4<br>2 | $^1A_1g\rightarrow{}^1B_1g$<br>$^1A_1g\rightarrow{}^1E_1g$ | | |

https://doi.org/10.30526/30.3.1617

### Table (4): TGA/DTG data for $[Cd(L)_2(H_2O)_2]$complex

| Stable up to°C | step | Dec. Temp. Initial-Final (°C) | DTG Temp. (°C) | Wt. of mass loss (calc)-found | Wt. of mass loss (calc)-found % | Reaction | Total mass loss% |
|---|---|---|---|---|---|---|---|
| 78 | 1 | 78-193 | 138 | (0.6594)-0.5700 | (3.471)-3.000 | - $2H_2O$ | (87.912)<br>88.66 |
| | 2 | 193-319 | 296 | (7.9515)-8.1624 | (41.85)-42.960 | -($CS_2$+ $C_{14}H_{11}N_3OS_2F_3$) | |
| | 3 | 319-415 | 383 | (5.8387)-5.6335 | (30.73)-29.65 | - ($CS_2$ + $C_{12}H_8NOF_3$) | |
| | 4 | 415-578 | 484 | (2.2535)-2.4795 | (11.861)-13.05 | - $C_6H_7N_2O$ | |
| | residue | 578 ≤ | - | (2.2967)-2.5346 | | CdO | - |

### Table (5): Bacterial activity of ligand and its complexes

| **Compounds** | ***E. coli*** (G−) | ***P. aeruginosa***(G−) | ***B. stubtilis*** (G+) | ***S. Aureus (G+)*** |
|---|---|---|---|---|
| NaL | 13 | _ | _ | 16 |
| $[Co(L)_2(H_2O)_2]$ | 16 | 30 | 26 | 26 |
| $[Ni(L)_2(H_2O)_2]$ | 15 | 32 | 28 | 29 |
| $[Cu(L)_2(H_2O)_2]$ | 17 | 25 | 24 | 22 |
| $[Zn(L)_2(H_2O)_2]$ | 18 | 23 | 22 | 23 |
| $[Cd(L)_2(H_2O)_2]$ | 17 | 27 | 26 | 22 |
| $[Pd(L)_2]$ | 15 | 24 | 27 | 22 |

https://doi.org/10.30526/30.3.1617

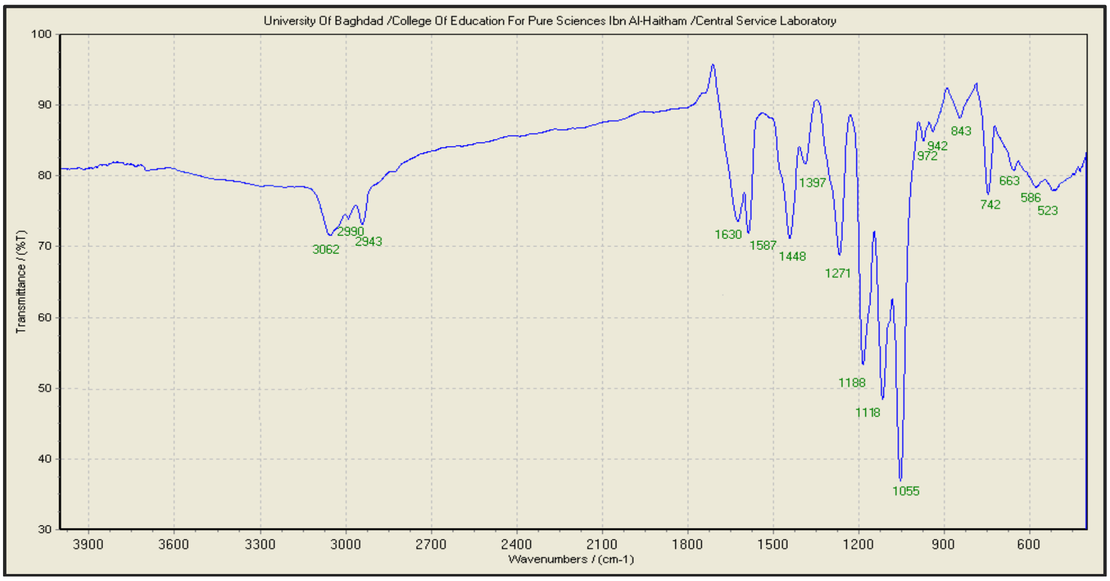

Figure (1): FTIR spectrum of NaL ligand

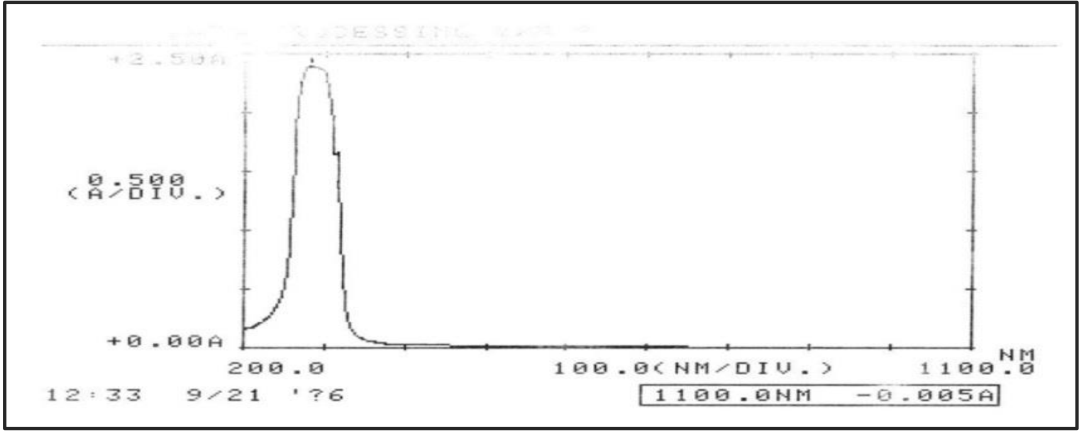

Figure (2): Electronic-spectrum of NaL ligand in DMSO solution

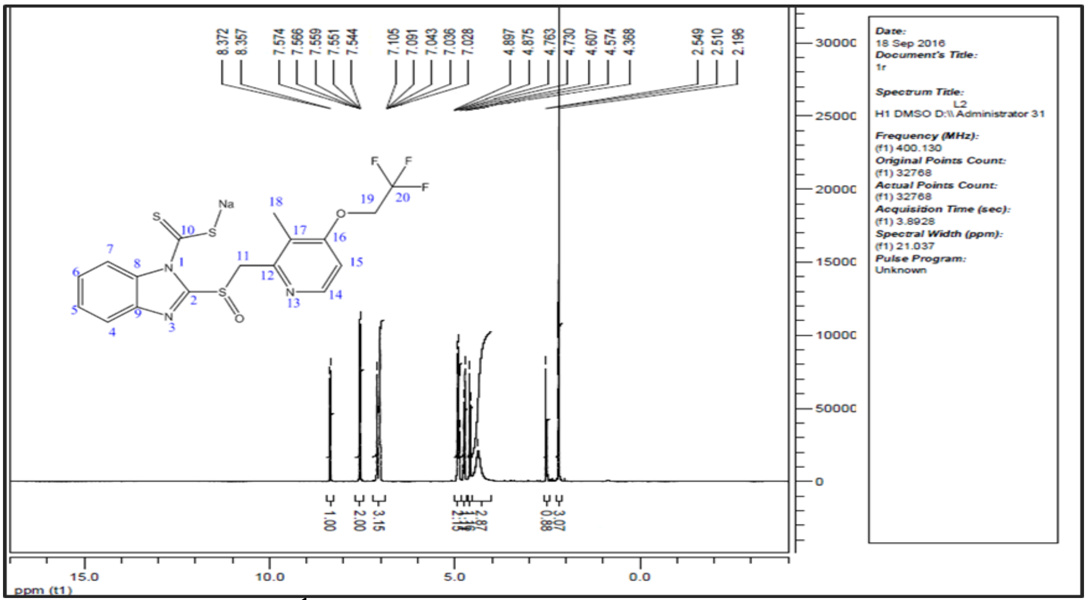

Figure (3): $^{1}$H-NMR-spectrum of NaL ligand in DMSO-d6

https://doi.org/10.30526/30.3.1617

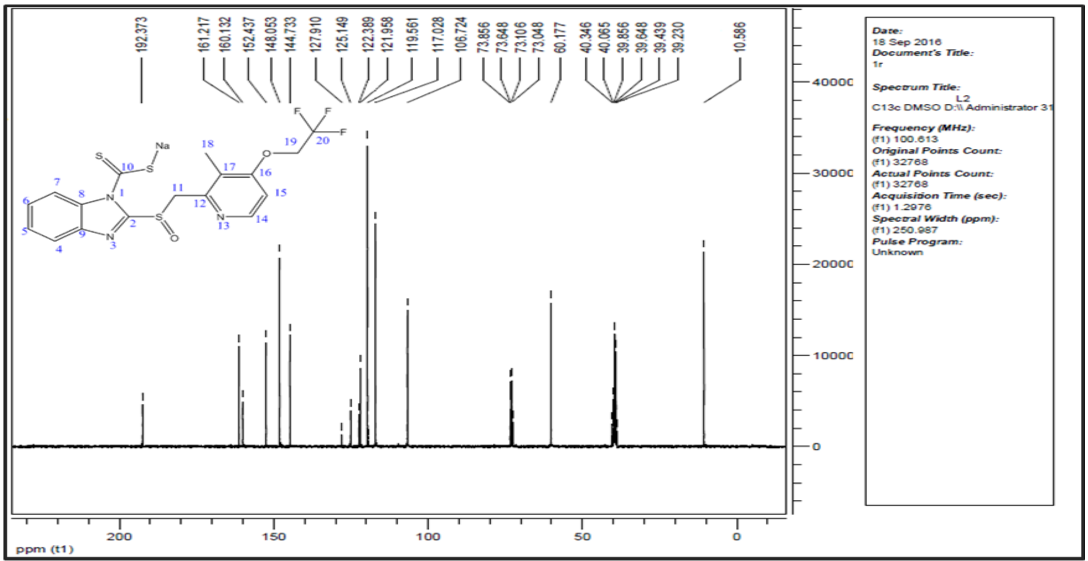

Figure (4): $^{13}$C-NMR-spectrum of NaL ligand in DMSO-d6

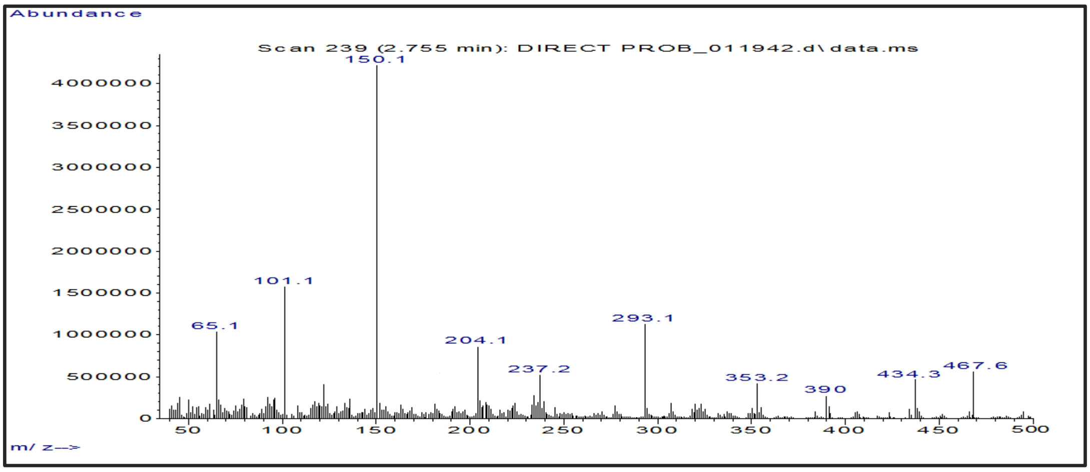

Figure (5): Mass-spectrum of NaL ligand

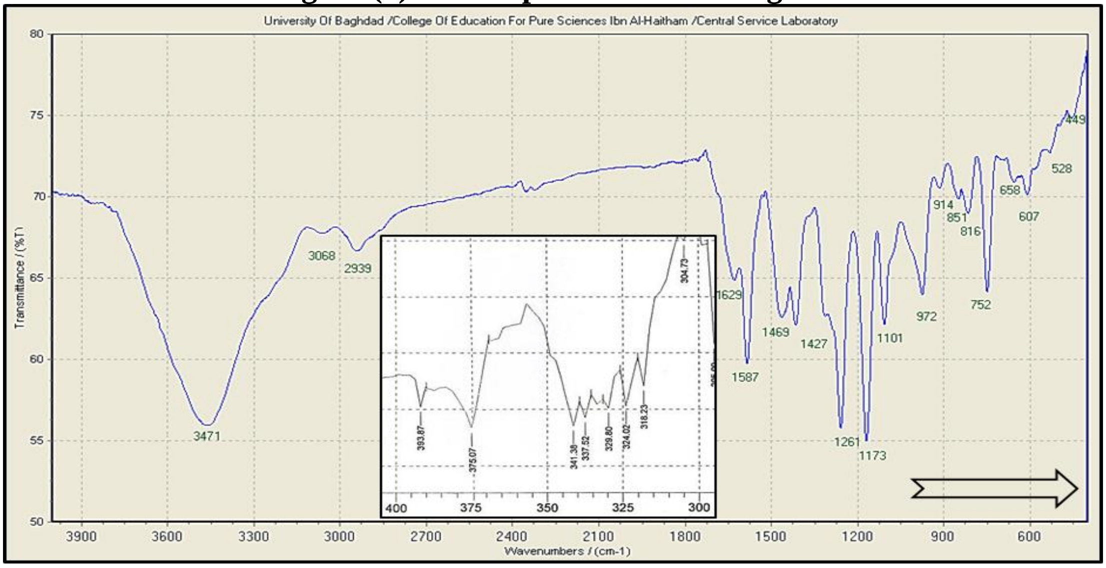

Figure (6): FTIR-spectrum of $[Co(L)_2(H_2O)_2]$ complex

https://doi.org/10.30526/30.3.1617

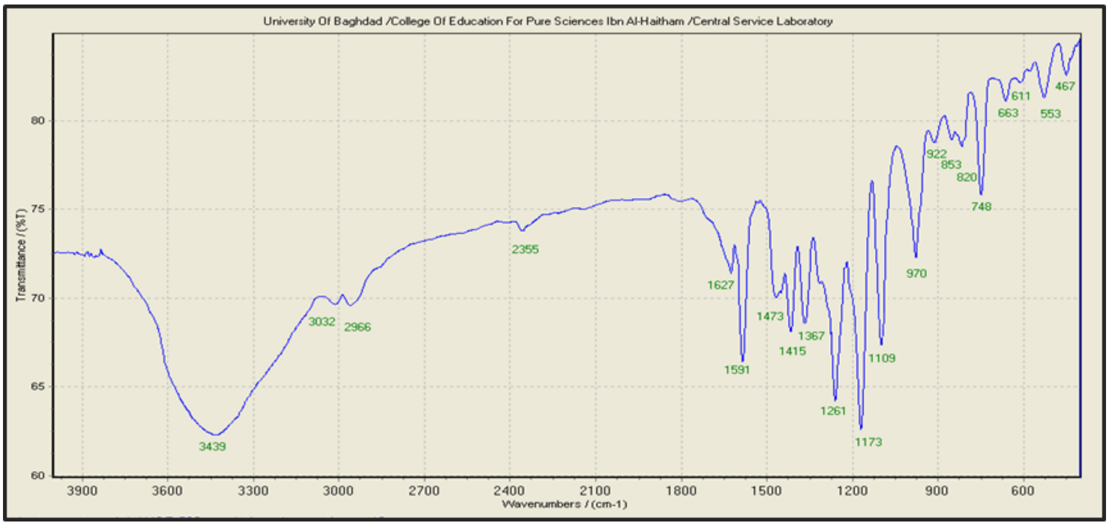

Figure (7): FTIR-spectrum of $[Ni(L)_2(H_2O)_2]$ complex

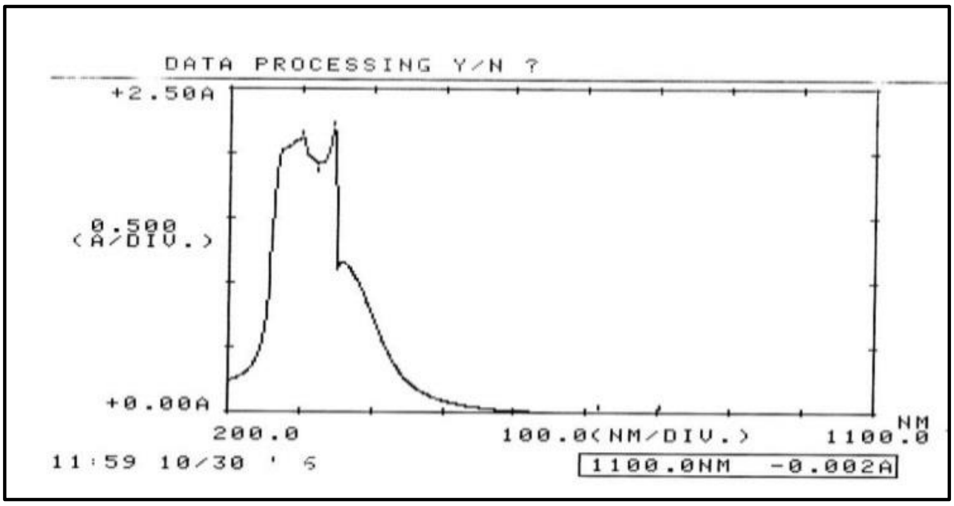

Figure(8): Electronic spectrum of $[Pd(L)_2]$ in DMSO solution

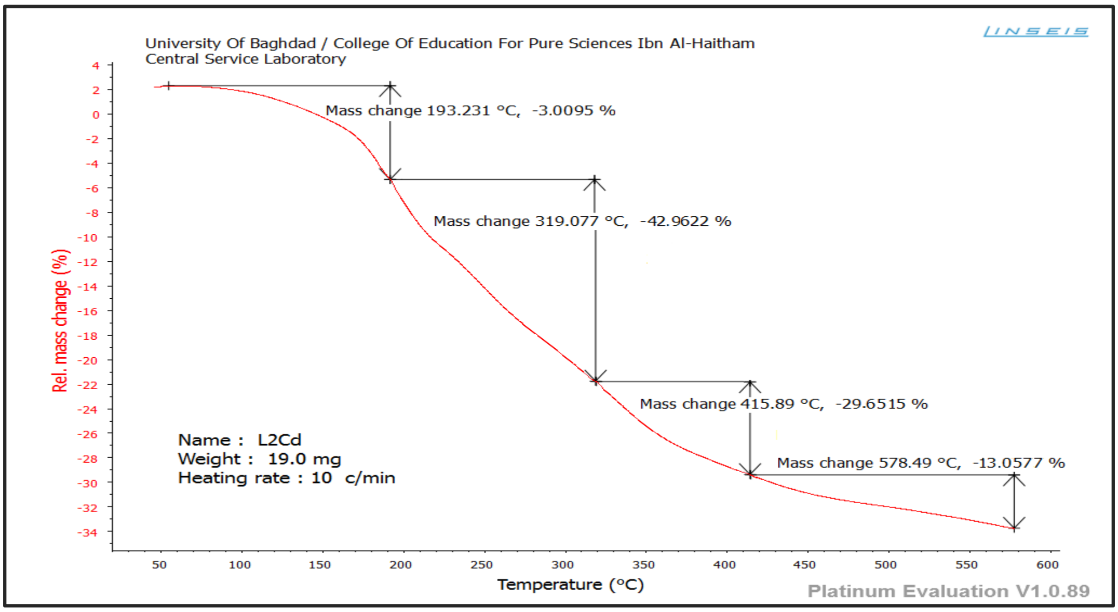

Figure(9): TGA for $[Cd(L)_2(H_2O)_2]$complex in helium atmosphere

https://doi.org/10.30526/30.3.1617

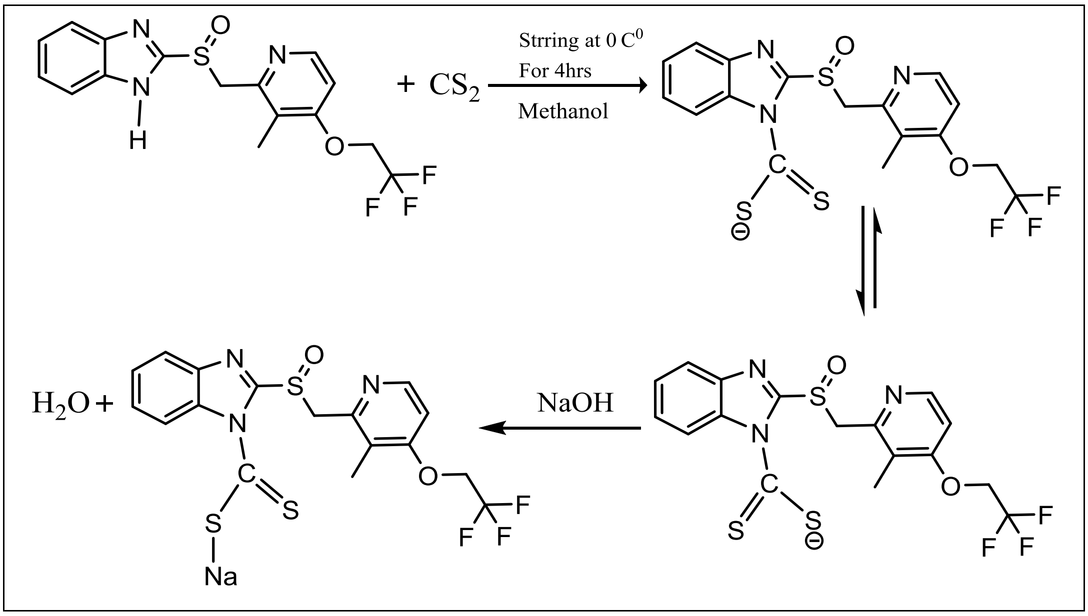

**Scheme(1) :Synthesis route of NaL ligand**

https://doi.org/10.30526/30.3.1617

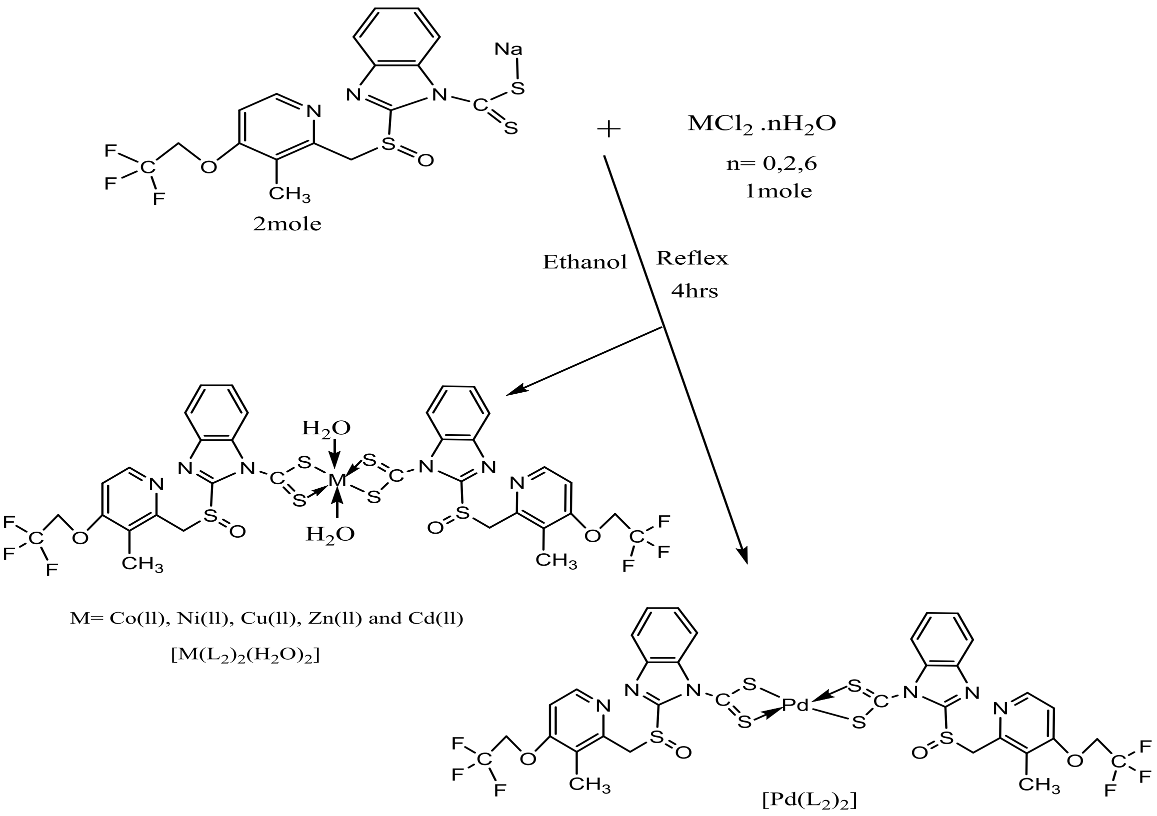

**Scheme (2): Synthesis route of NaL complexes**

https://doi.org/10.30526/30.3.1617